Central European Journal of Energetic Materials, **2015**, *12*(3), 473-486
ISSN 1733-7178
e-ISSN 2353-1843

Implementation of Sapper-Blast-Module, a Rapid Prediction Software for Blast Wave Properties

Piotr W. SIELICKI [*], Michał STACHOWSKI

Poznan University of Technolog,
Institute of Structural Engineering,
Marii Skłodowskiej-Curie 5, 60-965 Poznań, Poland
[*] *E-mail: piotr.sielicki@put.poznan.pl*

Abstract: This paper reports on a new methodology to provide rapid predictions of blast loading from spherical TNT charges. The rapid prediction method described has been coded by the authors into the open source Scilab and Matlab programming languages. The approach presented is based on experimental data and empirical formulae collected in official standard Unified Facility Criteria. The correctness of the results is proved for the explosion of spherical, condensed charges, both in free air space and as surface explosions. By taking a standard engineering approach, any engineer should be able to predict the primary features of explosive loading and take it into account during their design processes. This code is a part of the module called Sapper-Blast. Moreover, the main part of the paper also includes a comparison of the outcome with numerical verification. The results are presented for TNT spherical charges. The numerical consideration is performed using ABAQUS Explicit code. The results allow an informed assessment of the basic properties of an explosion for an equivalent mass of TNT for any kind of condensed, spherical charge. In addition, the approach presented demonstrates the overestimation of official results due to numerical approaches.

Keywords: explosion, blast loading prediction, numerical analysis

1 Introduction

It is possible to perform an assessment of the safety of a structure under explosive loading, but this aspect of safety is not considered in worldwide standards. Nevertheless, there are many methods which give a diverse range of results. These depend strongly on the insight of the designer or researcher and on the fields of interest, such as highly dynamic behaviour [1], which are taken into account. In fact, only a few countries have introduced explosive loading in official codes. Nevertheless, the most popular is the US Standard Unified Facility Criteria [2]. The present work presents a rapid assessment methodology which is based in particular on the Unified Facility Criteria. However, the authors will focus on the credibility and the real safety factor resulting from this approach. There are many factors which influence strongly the proper assessment of blast loading. The shape of the charge, the location of the ignition point and weather conditions are important for blast outcomes. Because of these reasons the safety factor so called "mass increasing" must be taken into account. "Mass increasing" means that one can use for the calculation exaggerated data, in respect to the real explosive parameter, *e.g.* 120% (safety factor = 1.2) of the mass of the charge. As a result, applying of this factor gives highest loading. Moreover, the complete profile of blast pressure with time always has the classical form, as presented in Figure 1a. This loading is generated by the pressure changes, which initially occur over only a few microseconds, released during chemical conversion inside the explosive volume. Moreover, the variation in overpressure in free air space for a surface explosion can be affected by the presence of ground reflections. In Figure 1a is the overpressure history, also called the air blast pressure. The term stand-off is used to denote the separation from the charge centre of any particular measurement point.

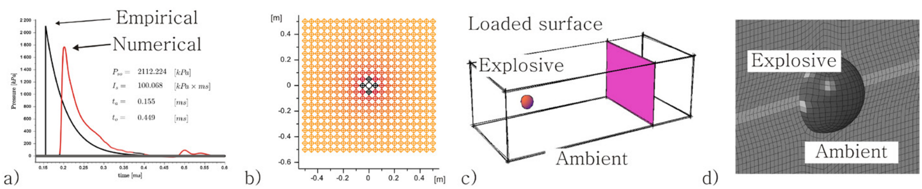

Figure 1. Views of the loading surface: a) pressure-time relation for a selected point on the loaded surface, empirical *vs*. finite elements method (FEM) solution, b) loaded surface, c) air volume with the location of a virtual air plane and explosive, d) numerical model in ABAQUS CAE.

Following the initiation of the explosion, after the arrival t_a, the pressure suddenly increases to a peak value P_{so} which exceeds the ambient pressure P_0. Subsequently, the pressure decays to P_0 in time t_0, then reaches the underpressure $P_{\overline{so}}$, and finally returns to the barometric value at time $t_{\overline{0}}$. The sum of the over- and under-pressure times is called the duration time T. The value of P_{so} is usually referred to as the peak side-on overpressure or incident peak overpressure (see Figure 2).

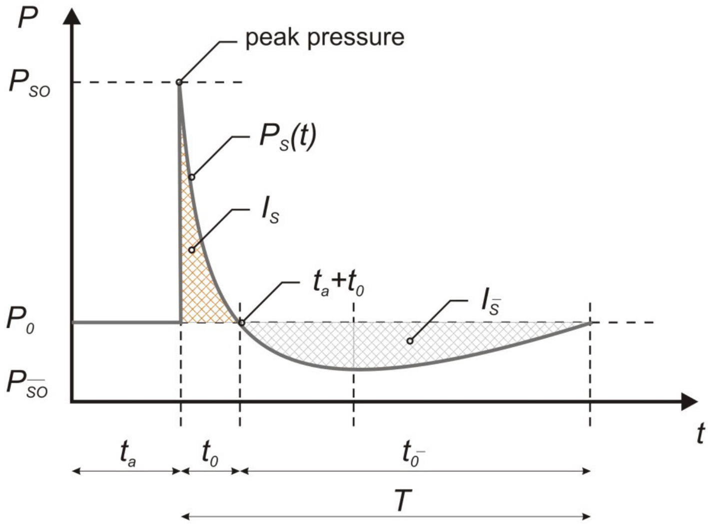

Figure 2. Standard blast pressure as a function of time.

A knowledge of the instantaneous pressure changes and the duration of the positive phase allows one to calculate the blast impulse of an explosion I_s. It may be noticed that the positive phase and its impulse are highly important for the structural strength of any kind of obstacle. In fact the blast resistance capacity of any structure can be presented as lying along a curve drawn in P-I space [2, 3].

2 Prediction of Explosive Properties

2.1 Introduction

It is possible to obtain the primary properties of an explosive loading using tabular data collected in standards. However, a primary question which must also be addressed deals with the possibility of reflections of the blast wave. It is noticed that the pressure wave could be reflected before it reaches the main obstacle, *e.g.* from the ground surface. Furthermore, these reflections intensify the pressure, and the final result could be significantly different from a purely free air explosion. In the official codes [2, 4-6] data exist for both free air and surface explosions. This paper includes both cases. The first one represents a purely theoretical phenomenon. The second is a hemispherical detonation. This is the typical scenario where the charge is located directly on the ground. It means that the pressure generated during the detonation reaches the ground. The reflected pressure wave then goes through the air and loads the obstacle.

Additionally, both of these approaches must be considered during standard engineering computations. The data presented in official standards [2, 5] come directly from actual explosive tests. Moreover, all of the values have been approximated by simple empirical forms. These outcomes were then transferred by the authors of this paper into rapid prediction software, thus generating the typical properties of explosive pressure action. Typical results are presented in Figures 1a and 1b.

The preliminary results were obtained for an explosion of a 1 kg TNT charge placed at a 1 m stand-off. Moreover, the shape of the charge and point of ignition were fixed to be spherical and detonated centrally respectively. The virtual air plane, *i.e.* the loaded area of interest was fixed at 1×1 m^2, which is partially represented by the axes in Figure 1b.

Detailed views of the loaded air section allows maps of the different properties to be presented, according to [2]. These are: R − stand-off distance, W − charge weight, Z − scaled distance, P_r − peak positive normal reflected pressure, P_{so} − peak positive incident pressure, I_r − unit positive normal reflected impulse, I_s − unit positive incident impulse, t_a − time of arrival of blast wave, t_0 − duration of positive phase of blast pressure, U − shock front velocity, L_w − wave length of positive pressure phase, $P_{\bar{r}}$ − peak negative normal reflected pressure, $P_{\overline{so}}$ − peak negative incident pressure, $I_{\bar{r}}$ − unit negative normal reflected impulse, $I_{\bar{s}}$ − unit negative incident impulse, $t_{\bar{0}}$ − duration of negative phase of blast pressure, $L_{\bar{w}}$ − wave length of negative pressure phase. Selected primary blast wave properties, calculated by Sapper-Blast-Module, the rapid prediction software, are plotted in Figure 3.

The authors' code allows for an optional plot of selected blast wave parameter as a function of time. The proposed method gives a rapid opportunity for blast assessment and verification of the influence of many important factors. An additional feature of the empirical code allows for matching only the part of the ambient space where a selected parameter reaches a defined condition. This feature is important for the consideration of only one parameter of the blast phenomenon. For example, where the overpressure is in excess of 350 kPa (see Figure 3a), the time of arrival is over 0.7 ms (see Figure 3e) and the positive reflected impulse is in excess of 350 kPa·ms, see Figure 3g. Furthermore, the programmed procedure allows the blast loading conditions to be exported to a text file in two different set of units, SI or US. In fact it allows other simulations of the structural response to be performed using different codes, but with the same loading conditions. The typical course of the overpressure *vs.* time is presented in Figure 3b.

2.2 Numerical solution

Credible modelling of the rapid pressure evolution passing through ambient air and reaching obstacles is a complex challenge, and must include an explicit numerical approach. According to the finite elements method, a high density mesh of Eulerian finite elements is necessary to obtain proper results. It has been numerically proved [3] that the critical size of the FEM mesh must be lower than 5×10^{-3} m for explosion analysis where the scaled distance is about 1.5 $m\cdot kg^{-0.33}$ and the stand-off below 1 m.

Moreover, the equations for the motions that are necessary to describe the blast waves of an explosion are complex. This means that it is not possible to obtain the analytical solution of a spatial explosion phenomenon, and researchers turn towards a numerical approach, *i.e.* finite elements modelling, as a highly elaborate tool for solving blast challenges. These equations were first solved by Brode [7] and then verified numerically by Kingery [8]. Additionally, such problems frequently incorporate the analysis of the target loading and its response. In this paper the numerical FEM analysis was performed with the use of the finite elements code ABAQUS Explicit v.6.13 [3, 9]. The primary study assumed the propagation of the explosive pressure wave through a pure medium such as ambient air, see Figures 1c and 1d. Implementing the set of equations [3, 9-12], it is possible to evaluate the problem using the following system of equations:

$$
\begin{array}{ll}
\text{Equation of motion} & \sigma_{kl,l} + \rho f_k = \rho \ddot{u}_k \\
\text{Geometric equation} & \varepsilon_{kl} = 0.5(u_{k,l} + u_{l,k}) \\
\text{Equation of state} & p = p(\sigma, E_m) \\
\text{Stress boundary conditions} & \sigma_{kl} n_l = \hat{t}_k \\
\text{Displacement boundary conditions} & u_k = \hat{u}_k \\
\text{Initial conditions} & u_k = \hat{u}_k^0,\ \dot{u}_k = \hat{\dot{u}}_k
\end{array}
\tag{1}
$$

where: $\sigma_{kl,l}$ − stress tensor component; ε_{kl} − strain tensor components; $u_{k,l}$ − derivative component of displacement; n_l − the direction; $\hat{t}_k$ − stress vector; $\hat{u}_k^0$, $\dot{u}_k$ − displacement and velocity components at the edge of the body; ρ − density and E_m − specific energy. Nevertheless, Equation (1) allows one to solve the linear dynamic problem. The nonlinear dynamic problems, which include the explosion phenomenon, must be solved with some additional modifications introduced to the set of Equations (1). In this work, the solution of Equation (1) was obtained using explicit FEM. The ambient air was modelled as an ideal gas (IG), see Equation (2):

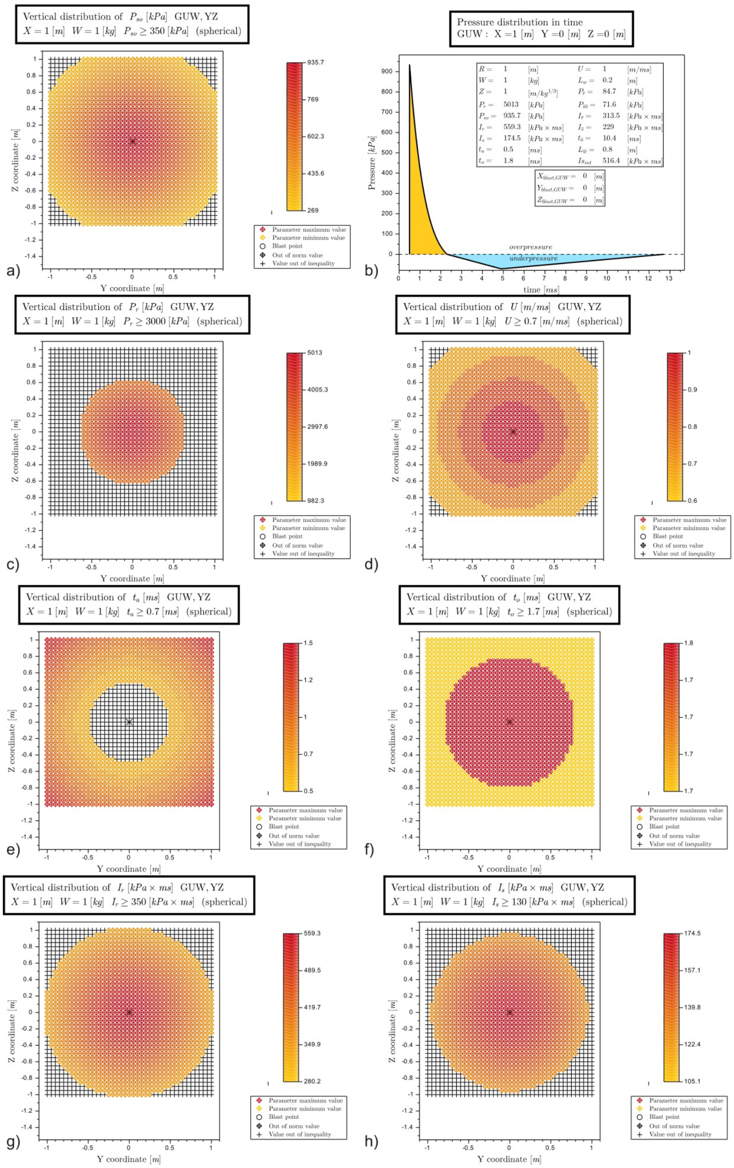

Figure 3. Primary parameters of the blast wave on a 2×2 m^2 virtual plane from a spherical explosion of 1 kg TNT at 1 m distance: a) positive pressure, b) pressure *vs.* time, c) reflected pressure, d) shock wave velocity, e) arrival time, f) positive phase duration, g) reflected impulse, h) positive incident impulse, as calculated by the rapid prediction software.

$$p + p_a = (\gamma - 1)\rho E_m,$$
$$p + p_a = \rho R(T - T^Z). \quad (2)$$

Moreover, these relations depend on the specific internal energy E_m. In order to most accurately reflect reality, the air must be initialised with both a greater than zero internal energy and an initial ambient pressure. The following equations, with $\gamma = 1.4$, are used for ideal diatomic gas modelling. p_a is the ambient pressure, ρ is the initial air density, R is the universal gas constant, and T^Z is absolute zero on the temperature scale being used. The value of the ambient pressure is represented by pressure at sea level.

The important material parameter is the specific energy, as presented in Equation (3), which changes with temperature and can be expressed in the following form:

$$E_m = \int_0^{T-T^z} c_v(T)dT + \int_{T_0-T^z}^{T-T^z} c_v(T)dT, \quad (3)$$

where: the first part is called the initial specific energy at room temperature $T_0(E_{m0})$ and c_v is the specific heat at constant volume. This discretisation of the surrounding air is very important while the material model includes the principles presented in Equation (1). The critical size of the Eulerian finite elements was fixed and equal to 0.005 m. These assumptions were adopted for the following two domains: ambient air and charge domains.

The behaviour of condensed charges, introducing products of detonation, is highly complex and depends strongly on the detailed features of each explosive. Nevertheless, a description of the classical blast loading can be obtained using only the explosive itself, *i.e.* TNT. This approach is tricky because of the fact that for other condensed charges, the peak pressures could be the same as for TNT, but the impulses and phase durations could be very different. However, this approach is widely used, especially when considering this phenomenon numerically. The present authors have therefore focused on TNT charges, and numerical as well as experimental studies have been performed for this kind of explosive [3, 13]. A credible description of the blast loading is an important point for any kind of numerical approach, as well as for analytical studies.

The widely-used Jones-Wilkins-Lee (JWL) equation of state [3], as presented in Equation (4), was used to describe the expansion of the combustion products of TNT.

$$p = A\left(1 - \frac{\omega\rho}{R_1\rho_0}\right)\exp^{\left(-R_1\frac{\rho_0}{\rho}\right)} + B\left(1 - \frac{\omega\rho}{R_2\rho_0}\right)\exp^{\left(-R_2\frac{\rho_0}{\rho}\right)} + \omega\rho E_m \quad (4)$$

The JWL equations describe the pressure generated by the chemical energy of the condensed explosive. The constitutive properties: A, B, R_1, R_2, are only available by laboratory testing. E_m is the internal specific energy per unit mass and ρ is the instantaneous density of the detonation products. The initial ratio of ρ to ρ_0 used in the JWL equation is assumed to be unity. Table 1 gives the properties for TNT and the ambient domains.

The primary purpose for the implementation of the numerical solution was to allow verification of the methodology presented in the official codes. Furthermore, it allowed a credible approximate solution of the explosion blast wave and its propagation. It is possible that the empirical approach implemented into the authors' open code has given over-estimated values due to the numerical process. A visual representation of the numerical model is presented in Figure 4.

This picture represents a spatial ambient space of $2 \times 2 \times 2$ m^3 with the spherical explosive embedded inside. A numerical algorithm was created which generated a wide range of examples for analysis.

Table 1. Material properties for TNT and air media [3]

JWL properties for TNT Explosive		
A	3.4×10^{11}	Pa
B	3.75×10^{9}	Pa
R_1	4.15	–
R_2	0.9	–
E_m	4.5×10^{6}	$J \cdot kg^{-1}$
ω	0.35	–
C_d	6930	$m \cdot s^{-1}$
ρ_0	1630	$kg \cdot m^{-3}$
IG properties for Ambient Air		
R	287	$J \cdot (kg \cdot \mathrm{K})^{-1}$
ρ	1.297	$kg \cdot m^{-3}$
p_a	101325	Pa
E_m	0.193×10^{6}	$J \cdot kg^{-1}$
T^z	0	K
T_0	288.4	K
c_v	717.6	$J \cdot (kg \cdot \mathrm{K})^{-1}$

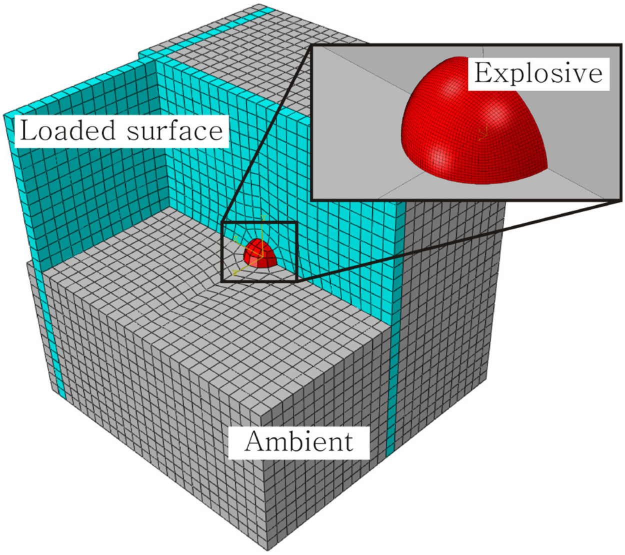

Figure 4. A representative model for the numerical solution of the detonation and explosion phenomena.

3 Results

A methodology for the prediction of blast pressure loading has been presented above. The implementation of this was programmed by the authors into the Scilab and Matlab programming languages. Nevertheless, the results obtained must be verified by actual or numerical comparisons. In fact, solutions were obtained from the numerical solution for the blast wave approach, both in free air and for surface explosions, for many combinations of the input factors. Finally, 480 combinations for TNT and C4 explosives were set up of. Additionally, two other features were taken into account *viz.* different stand-off distances and the mass of the charge. In all of the cases considered, the shape of the explosive was spherical.

Typical results were plotted on the virtual plane of the air slice with constant dimensions 2×2 m^2. This plane was located at a stand-off of 0.94 m. Furthermore, for the surface explosion the height of the TNT explosive was 0.16 m above the ground surface. The explosive mass was 11.8 kg.

Of all of the 480 comparisons, only one is presented here, that which gave the worst convergence. The numerical calculations were computed in ABAQUS Explicit. The verification included the standard (free air) and surface solutions of the detonation process and the propagation of the pressure wave through ambient air. The behaviour of the two surrounding media was described by two equations of the states, as presented in the previous part of this work. The shape of the explosive was fixed to be spherical, with a central ignition point. The finite elements describing the ambient as well as the charge were purely Eulerian. 10^5 finite elements described the spherical explosive, and *ca.* 4×10^6 elements for the ambient air. The surface explosion considered the ground surface as represented by fixed nodes. In addition, the initial conditions: ambient pressure, temperature and specific energies, were used.

The primary comparison presents the peak pressures and impulses of the overpressure which exist in the free air slice. In addition, the pressure time relation is presented for a virtual point in the air, located 0.94 m from the detonation centre, for both examples. Comparisons of the results obtained for the rapid prediction *vs.* the numerical verification, are presented in Figure 5 for the free air, and in Figure 6 for the surface explosions, respectively. It is important to emphasize that the graphical view of the impulses, Figures 5b and 6b, was not possible in ABAQUS. In fact, the authors obtained numerically the pressure-time curves for all of the integration points for elements located on the resulting plane. These curves were then integrated in order to calculate the impulse values. These solutions were transferred into the Scilab/Matlab code for comparison with the rapid prediction software.

Figure 5a shows the overpressure map on the virtual plane. This solution was obtained using the rapid prediction algorithm prepared by authors. A comparable study was done using the FEM approach. In addition, a perpendicular plane is shown which allows tracking of the blast wave propagation in the air, before it reaches the resulting plane. A study of these results allows a detailed assessment of the pressure zones on the obstacle surface. The maximum values of the overpressure were 5350 and 5050 kPa for the rapid prediction and numerical solutions respectively. However, the impulses, calculated by the two methods, are very close in value, at 311 and 308 kPa·ms, respectively. The pressure maps were convergent.

The results for a surface explosion, where the charge is located just above rigid ground are presented in Figure 6. A comparison of the overpressures allows any discrepancies to be found. However, on comparing the pressure for separate points with adequate integration points, the results were found to be similar. For the points located just above the ground, differences were observed. The same relations exist when the positive impulses are compared.

Furthermore, in Figure 6c, where the pressure-time curves are compared, there exists a phase shift on the time axis. This is caused by the initial boundary conditions which reflect the ground surface. The measurement of the results for the finite elements, which are located near to the boundaries, introduce errors. Nevertheless, the average peak pressure and positive impulse are well obtained. The surface explosion generates the overpressure peak. These were 6420 and 6750 kPa for the authors' rapid prediction method and the FEM solution, respectively. The corresponding impulses were 391 and 372 kPa·ms, respectively.

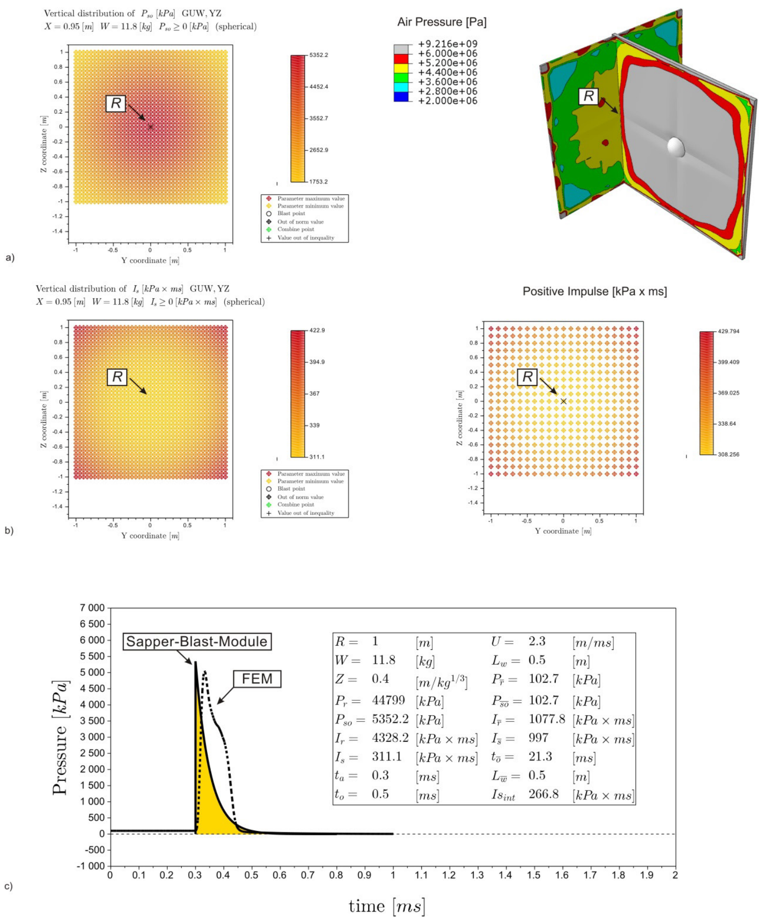

Figure 5. The free air explosion comparisons, with (on the left) the Sapper-Blast-Module prediction algorithm *vs*. (on the right) the numerical solution in ABAQUS, for: a) peak pressure, b) positive impulse, c) the pressure-time relation at the point R =1 m.

Additional blast wave properties are presented in Figures 5c and 6c. All of these features come from the official code [2, 5] and were transferred using the authors' algorithm to predict the average blast wave properties. The most important parameters deal with the reflected values of the overpressure and impulse, *i.e.* P_r, I_r. These data are considered during the design process for structures [3, 14-16].

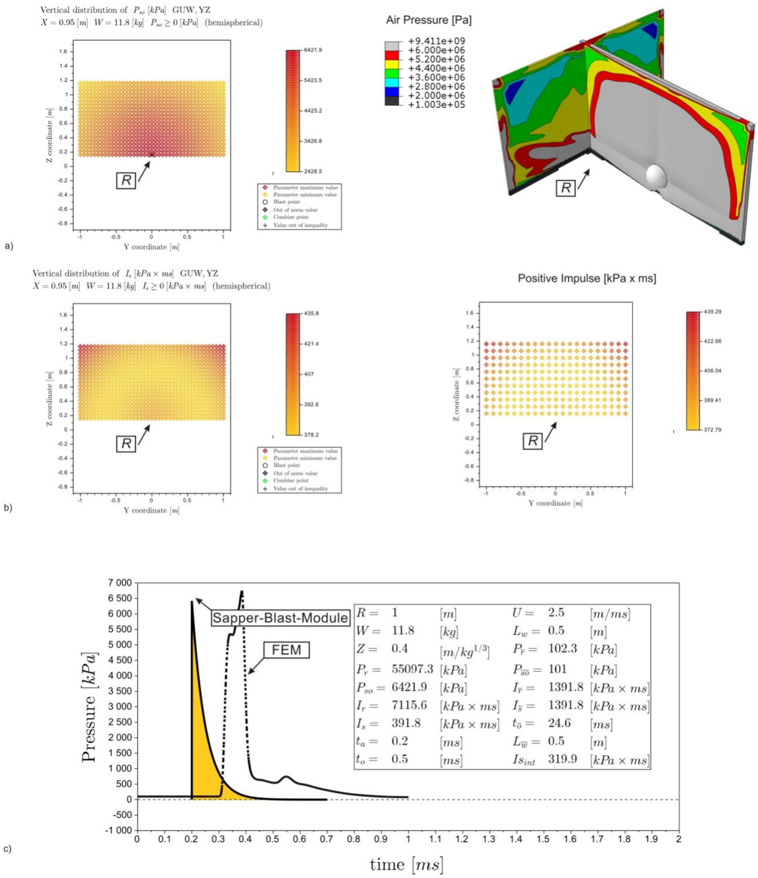

$R=$ 1	[m]	$U=$	2.5	[m/ms]
$W=$ 11.8	[kg]	$L_w=$	0.5	[m]
$Z=$ 0.4	[m/kg$^{1/3}$]	$P_{\bar{r}}=$	102.3	[kPa]
$P_r=$ 55097.3	[kPa]	$P_{\bar{so}}=$	101	[kPa]
$P_{so}=$ 6421.9	[kPa]	$I_{\bar{r}}=$	1391.8	[kPa × ms]
$I_r=$ 7115.6	[kPa × ms]	$I_{\bar{s}}=$	1391.8	[kPa × ms]
$I_s=$ 391.8	[kPa × ms]	$t_{\bar{o}}=$	24.6	[ms]
$t_a=$ 0.2	[ms]	$L_{\bar{w}}=$	0.5	[m]
$t_o=$ 0.5	[ms]	Is_{int}	319.9	[kPa × ms]

Figure 6. The surface explosion comparisons, with (on the left) the Sapper-Blast-Module algorithm *vs.* (on the right) the numerical solution in ABAQUS, for: a) peak pressure, b) positive impulse and (overlaid), c) the pressure-time relation at the point $R = 1$ m.

4 Conclusions

In this paper, the implementation of a rapid prediction method for the assessment of blast wave properties has been presented. This procedure was written by the authors into the open source code Scilab. The methodology introduced deals with the solution of average blast loading conditions on a virtual plane or at virtual points in ambient space. The results were verified by means of 480 worked examples, which were compared with numerical solutions. From these examples, the least favourable comparison, presented above, shows that the rapid prediction method produces predicted values for peak pressure, positive impulse *etc*., which are close to those predicted by the more time-consuming ABAQUS numerical code. However, the comparison presented so far is only for spherical TNT charges. The application to other types of the explosives *e.g.* C4 or PE4, would be possible, however, by introducing a reliable TNT equivalent factor [13]. The algorithm presented here therefore provides the engineer with the necessary overpressure and impulse predictions to perform a rapid assessment of the strength analysis of structural elements or to obtain the safety zones. Finally, the authors still recommend the introduction into such an analysis of a safety factor which increases the TNT mass equivalent of the charge by 22%. The solution provides maps where the overpressure *vs.* impulse conditions are experienced.

Acknowledgement
The authors would like to thank the Polish National Centre of Research and Development for their financial support, project UOD-DEM-1-203/01.

5 References

[1] Glema A., Łodygowski T., Sumelka W., Nowacki's Double Shear Test in the Framework of the Anisotropic Thermo-Elasto-Viscoplastic Material Model, *J. Theor. Appl. Mech.*, **2010**, *48*(4), 973-1001.
[2] *Design and Analysis of Hardened Structures to Conventional Weapons Effects*, Departments of the Army US Army Manual, UFC 3-340-01, **2008**.
[3] Sielicki P.W., *Masonry Failure under Unusual Impulse Loading*, Publishing House of Poznan University of Technology, Poznan, **2013**, ISBN 978-83-7775-274-6.
[4] British Standards Institution, Eurocode 6: *Design of Masonry Structures − Part 1-1: General Rules for Reinforced and Unreinforced Masonry Structures*, B EN 1996-1-1, BSI London, **2005**.
[5] *Structures to Resist the Effect of Accidental Explosions*, Departments of the Army US Army Manual, UFC 3-340-02, **2008**.

[6] DOE/TIC-11268, *A Manual for the Prediction of Blast and Fragmentation Loadings on Structures*, US Department of Energy, **1992**.
[7] Brode H.L., *Numerical Solutions of Spherical Blast Waves*, Defense Technical Information Center, **1955**.
[8] Kingery C.N., Bulmash G., *Airblast Parameters from TNT Spherical Air Burst and Hemispherical Surface Burst*, Ballistic Research Laboratory, **1984**.
[9] Abaqus 6.13, Documentation Collection, **2012**.
[10] Belytschko T., Liu W.K., Moran B., *Nonlinear Finite Elements for Continua and Structures*, Wiley, **2000**, ISBN 978-0471987741.
[11] Mazurkiewicz L., Małachowski J., Baranowski P., Damaziak K., Comparison of Numerical Testing Methods in Terms of Impulse Loading Applied to Structural Elements, *J. Theor. Appl. Mech.*, **2013**, *51*(3), 615-625.
[12] Niezgoda T., Małachowski J., Research of Elastomeric Protective Layers Subjected to Blast Wave, *Appl. Mech. Mater.*, **2011**, *82*, 680-685,.
[13] Rigby S.E., Sielicki P.W., An Investigation of TNT Equivalence of Hemispherical PE4 Charges, *Engineering Transactions*, **2014**, *62*(4) 434-435.
[14] Alia A., Souli M., High Explosive Simulation Using Multi-material Formulations, *Appl. Therm. Eng.*, **2006**, *26*, 1032-1042.
[15] Luccioni B., Ambrosini D., Danesi R., Blast Load Assessment Using Hydrocodes, *Engineering Structures*, **2006**, 28, 12, 1736-1744.
[16] Remennikov A.M., Timothy A.R., Modelling Blast Loads on Buildings in Complex City Geometries, *Comput. Struct.*, **2005**, 83, 27, 2197-2205.